We would like to sincerely thank both reviewers again for their valuable feedback and comments. We feel that the revisions suggested by the reviewers have greatly improved the manuscript. Our point-by-point responses are included below for each reviewer. In addition to the changes outlined below, we would also note two additional edits that were made to the manuscript without specific requests/concerns from the reviewers. Both of these edits are minor and do not alter any of the key findings results that we present in this work.

1. **We have added the TROPOMI-based estimates from East et al. (2025) into our comparison plots and mentions of their results throughout the text. This dataset from East et al. (2025) provides a recent high-resolution global emissions estimate for 2023 which is valuable dataset to add for intercomparisons.**

2. **We have revised Figures 5 and 6 to include less text and clearer heatmaps displaying residual emissions. Only aesthetics were altered in the revision of these figures.**

Reviewer comments are highlighted in *black italic text*

Our written responses are shown in bold blue text

Current text in the manuscript is shown in blue text

Added text in the manuscript is shown in red text

Response to Reviewer #1

Specific Comments

Point #1: *[Page 5, lines 151–154] In your discussion of the sensitivity study methods, the comparison between mean and median emission rates per common global grid cell may be unstable. In Region A, there are at most nine independently calculated emission rate estimates per grid cell, whereas in Region B there are at most three, with other regions falling somewhere in between. With sample sizes this small, estimates of either the mean or the median at the grid-cell level are inherently unstable, and the addition of a single new observation could dramatically alter the mean or median value of the grid cell emission rate. I would appreciate either further clarification of what this comparison is intended to demonstrate, or an exploration of an alternative approach. For example, you could perform a bootstrap analysis in which the common global grid-cell value is repeatedly sampled from the available emission estimates within each grid cell, and then show where the basin-wide mean- and median-based calculations fall within the basin-wide bootstrapped distribution (i.e., similar to the bootstrapping algorithms presented in Appendix B).*

The reviewer is correct to point out that the aggregation of a small number of individual MethaneSAT scenes can produce unstable results at the grid-cell level, and we have taken several steps to explain this uncertainty. We add additional text to highlight that the aggregated MethaneSAT emissions products are not meant to be interpreted on a single cell basis since any single cell carries a large amount of uncertainty, but rather as parts of a larger sum, which in turn will reduce uncertainty in the estimates. We highlight this process and the proper interpretation of the aggregated MethaneSAT estimates in Sections 2.2 and 2.4, including newly added considerations for seasonal representativity. Single scene MethaneSAT estimates are calculated using 4,000 plausible emission estimates for every single emissions cell, from which the mean is used to represent the emissions for that single scene. We have clarified the text in the manuscript to better highlight this process

As an additional test of sensitivity, we've calculated the resulting variation in the MethaneSAT emissions estimates after removing single scenes from the aggregation process, which offers some insight into the impacts of including new scenes to the aggregated emissions. The resulting sensitivity analysis finds a maximum change in emissions of +17% for the Amu Darya – TKM region, with an overall absolute average variation of 5% across all 33 scenes.

We believe that this new sensitivity analysis, in addition to further clarification in the main text that aggregated individual MethaneSAT scenes do not inherently represent annual emissions estimates, address the main concerns of the reviewer.

We have made the following changes in the main manuscript and SI:

Lines 145 – 151: "Individual MethaneSAT emissions estimates (i.e., a MethaneSAT scene or emissions map) represent methane emission estimates up to 28 hours back in time and vary in their spatial dimensions depending on the viewing geometry of the satellite. Nadir viewing observations produce up to ~220 km wide scenes while off-nadir observations produce up to ~440 km wide scenes. The MethaneSAT platform had an agile observing mechanism with off-nadir viewing at up to 40 degrees on one side of its observing track. We aggregate multiple MethaneSAT scenes together over the same regions to produce a spatially explicit estimate of methane emissions with increased temporal and spatial extents."

Lines 156 – 160: "We also test the sensitivity of MethaneSAT aggregated emissions estimates to the removal of single scenes and find that estimates are robust among the six regions (SI – Section 2, Fig. S12). We additionally consider any impacts from seasonal variability in our aggregated emissions estimates using 2022 monthly inversions data from TROPOMI (Pendergrass et al., 2025) to better compare to annual emissions estimates from top-down satellite inversions or bottom-up inventories (SI – Section 2)."

Lines 237 – 246: "Uncertainty in aggregated MethaneSAT emissions estimates is propagated using a Monte Carlo approach. Each emissions cell is represented by 4,000 samples drawn from its MCMC posterior distribution, reflecting mean-level uncertainty in the emissions estimate at that location. Where multiple emissions maps overlap a given cell, 4,000 combined cell-level estimates are generated by repeatedly drawing one value per map and averaging across maps. This Monte Carlo resampling procedure propagates uncertainty through the arithmetic mean without requiring assumptions about the functional form of the resulting distribution. This procedure is applied independently to all subregions

defined by unique combinations of overlapping emissions maps (Fig. S2). Uncertainty on the total dispersed area emissions is the 95% confidence interval on the total across all samples (n = 4,000), with an additional 20% uncertainty added to account for assumed uncertainty in the static parameters in the input GFS weather data used for the inversions."

Newly added section: SI - Section 2 "Aggregation of MethaneSAT scenes and seasonal variability"

Newly added Fig. S10:

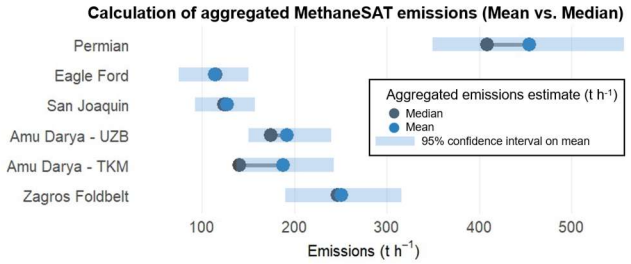

"Fig. S10: Differences in total methane emissions estimates after performing the aggregation of MethaneSAT scenes using the median or mean to calculate cell-level emissions from overlapping MethaneSAT scenes. Aggregated MethaneSAT total emissions are currently calculated using the mean for overlapping scenes. We find the largest difference between both approaches for the Amu Darya – TKM region, whereas the Zagros Foldbelt, San Joaquin, and Eagle Ford are relatively unchanged between approaches. Shaded blue bars represent the 95% confidence intervals of the current MethaneSAT aggregated estimates."

Newly added Fig. S12:

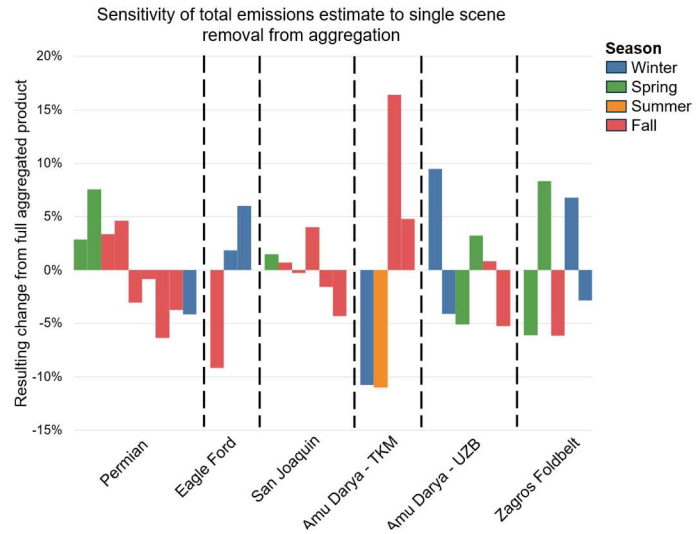

"*Fig. S12: Resulting variation in MethaneSAT aggregated emissions estimates after single scenes from the aggregation process. The bars are colored according to the season from which the MethaneSAT observations were obtained. The percentage differences are calculated based on the same spatial domain since the removal of scenes can vary the extent of the aggregated output boundary.*"

In addition, the text states that emission rates are being averaged per grid cell, a description that is also used in the caption of Figure S1. However, the label in the bottom-left panel of Figure S1 indicates that MethaneSAT observations are being averaged, rather than MethaneSAT regridded emissions. This discrepancy should be clarified. Furthermore, the figure does not specify what the error bars in Figure S1 represent.

We have corrected this instance and clarified language throughout the paper to differentiate observations versus the gridded methane emissions output from the inversion. We have also revised the in-figure text and caption of Fig. S1. We assume the reviewer was referring to Fig. S10 with regards to the error bars since there are none in Fig. S1. Our previous response addresses the lack of description for Fig. S10.

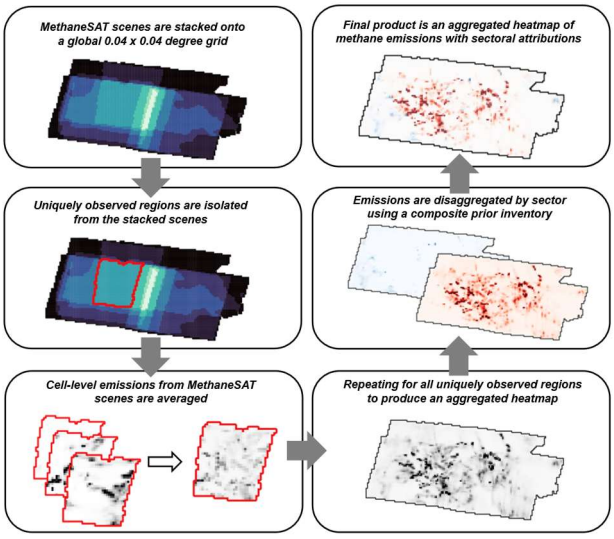

"Fig. S1: Diagram illustrating the methodology associated with the aggregation of multiple overlapping MethaneSAT emissions maps into a single regional estimate of methane emissions and the sectoral disaggregation of methane emissions derived from MethaneSAT observations."

Point #2: *[Page 6, lines 181-185] Here you describe the databases used as prior inputs for your regions and for non–oil and gas as well as oil and gas sources. While Figures S7 and S8 examine how varying the choice of prior database influences the sectoral attribution of emissions derived from MethaneSAT, a clearer explanation of how the specific combination of prior databases used for the final results was selected would be helpful. In particular, it would be useful to clarify how and why COMBO 26 in Figure S7 and COMBO 15 in Figure S8 were chosen as the final configurations.*

We agree that our selection of bottom-up inventories used in our composite prior inventories are not adequately described or justified. We have added new sections in the main text and SI that further detail our selection process for the composite prior inventories, now noting that we optimize our selection based on guidance from a literature-based proportion of oil and gas emissions that incorporates satellite-based observations and combinations of bottom-up inventories that are methodologically distinct (if available).

We hope the following modifications address the reviewers points:

Lines 187-193: "For any region and sector, we combine emissions estimates from two bottom-up inventories with Carbon Mapper distinct point sources to produce the composite dataset. For regions within the US, we use the EPA-GHGI and EDGAR as inputs for non-oil and gas sources, and the EI-ME and EDGAR for oil and gas sources. For regions outside of the US, we use CAMS v6.2 and EDGAR as inputs for non-oil and gas sources, and the GFEI v2 and EDGAR as inputs for oil and gas sources. Other combinations of these bottom-up inventories, and their impacts on the resulting sectoral breakdown of emissions, are provided in the SI (Fig. S7; Fig. S8) with further explanation in the SI – Section 1.1."

Lines 195-200: "To better account for regions where granular oil and gas infrastructure data is limited (i.e., regions outside of the US), we spatially aggregate oil and gas methane emissions estimates from the composite prior by a factor of four (i.e., from the native 0.1° x 0.1° resolution to 0.4° x 0.4°) while conserving the mass of emissions. A sensitivity test of this approach shows improved agreement in the sectoral proportions of emissions for non-US regions compared to a compilation of estimates from literature, while showing little to no improvement for regions in the US (SI – Section 1.2)."

Lines 623-626: "Sectoral attribution is applied as a post-inversion step using a composite prior inventory drawn from multiple spatially explicit datasets supplemented by global point source data from Carbon Mapper (2025). This approach improves sectoral allocation, especially for regions where information on oil and gas emissions data is sparse and information from one inventory can account for discrepancies in another (SI – Section 1.1, Fig. S5)."

Newly added sections in SI: SI Section 1.1: "Selection of inventories used for composite prior" and SI Section 1.2 "Oil and gas estimates for non-US regions"

Revised Figure S6 in the SI:

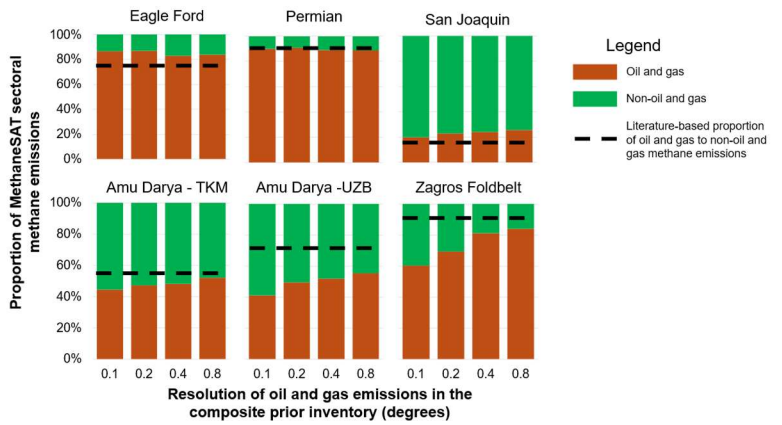

“Fig. S6: Impacts of varying the resolution of the oil and gas sectoral emissions from the composite prior inventory used to disaggregate methane emissions estimates from MethaneSAT. Results of the sensitivity test for all six regions are shown. The dashed black line indicates the literature-based proportion of oil and gas to non-oil and gas methane emissions in the six regions. For the US regions (top row), the chosen resolution used for sectoral disaggregation is 0.1 degrees. For non-US regions (bottom row), we use a resolution of 0.4 degrees.”

Revised Figure S7 and S8 in the SI:

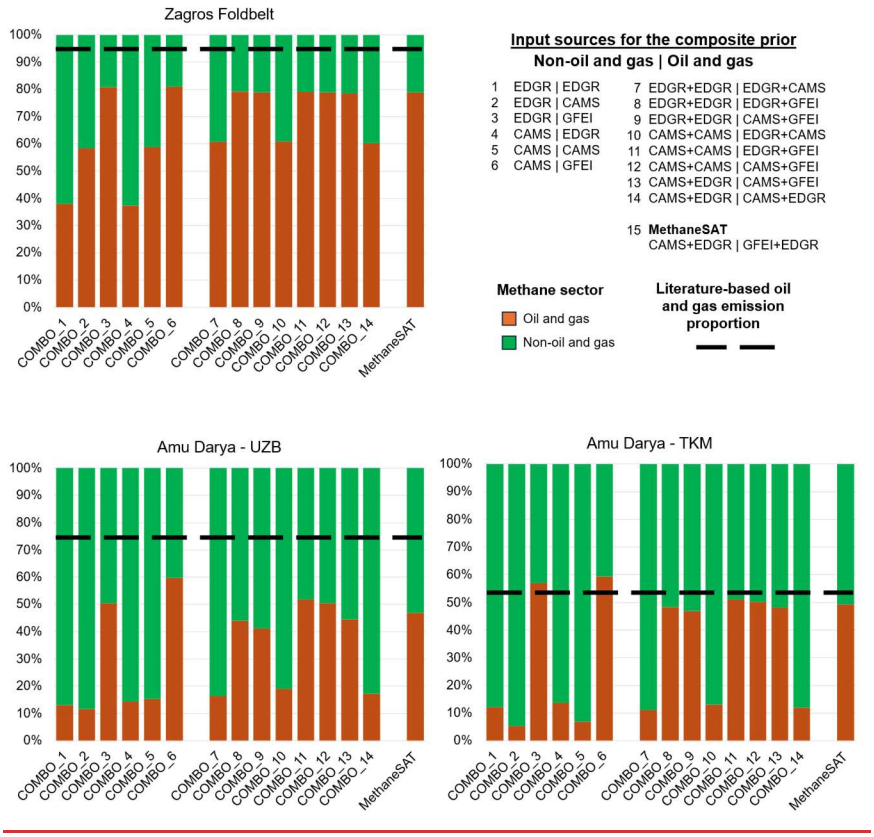

“Fig. S8: Impacts of varying the input data used in the stacked prior inventory to disaggregate methane emissions from the MethaneSAT observations for regions outside of the US. The impacts of the inclusion of Carbon Mapper point sources are also not shown. The dashed black line indicates the literature-based proportion of oil and gas to non-oil and gas methane emissions in the six regions.”

New Table S4 in the SI:

“Table S4: Studies and data sources used in the calculation of a literature-based proportion of oil and gas emissions which is explained in the SI Sections 1 and 2. Also indicated in the table is the respective name for the spatially-explicit methane emissions estimate (if applicable), a broad descriptor of the methodology used to obtain the methane emission estimate, a breakdown of the methane sectors included in the estimate, and the latest year represented within the dataset.”

Study	Data source name	Method	Sectors included	Latest year
(Maasakkers et al., 2023)	EPA-GHGI	Bottom-up	All	2018
(Omara et al., 2024)	EIME	Bottom-up	Oil and gas	2023
(Granier et al., 2019)	CAMS v6.2	Bottom-up	All	2024
(Crippa et al., 2024)	EDGAR_GHG_2025	Bottom-up	All	2024
(Scarpelli et al., 2022)	GFEI v2	Bottom-up	Oil and gas, coal	2019
(East et al., 2025)	-	TROPOMI	All	2023
(Shen et al., 2023)	-	TROPOMI	Oil and gas, coal	2019
(Worden et al., 2022)	-	GOSAT	All	2019
(Lu et al., 2023)	-	GOSAT	All	2019
(Nesser et al., 2024)	-	TROPOMI	All	2019

New Table S5 in the SI:

"Table S5: Literature-based estimates of oil and gas and non-oil and gas emissions within the spatial domains of all six regions. The resulting proportions are used to inform the selection process of inputs used for the composite prior, and to support the use of decreasing the resolution of bottom-up inventories."

Region	Literature-based oil and gas estimate (t/h)	Literature-based non-oil and gas estimate (t/h)	Literature-based proportion of emissions (oil and gas / non-oil and gas)
Eagle Ford	46.9	14.4	77 / 23
Permian	290	23.8	92 / 8
San Joaquin	16.1	82.7	16 / 84
Amu Darya - TKM	57.9	48.6	54 / 46
Amu Darya - UZB	94.4	32.4	74 / 26
Zagros Foldbelt	310	16.0	95 / 5

Point #3: *[Page 7, lines 217-218] You state that an assumed methane composition of 80% in natural gas was used for all intensity metric calculations. Did you perform a sensitivity analysis to assess how varying this assumed methane concentration affects the resulting intensity estimates? In addition, are there datasets or studies that could be used to sample basin specific methane concentrations in natural gas? For example, Burdeau et al. [2025] provide basin-level produced gas composition estimates for two of the U.S. basins included in your study, albeit for a slightly earlier timeframe.*

Since we use methane composition in the denominator of our gas-normalized intensity computations for our team's analyses, the intensity scales inversely with the methane

composition. The changes in intensity are dependent on the ratio of differing methane compositions, not the percentage change in the composition. For the 80% -> 70% change in composition assumption example, which is a 12.5% decrease in the composition estimate, the increase in the intensity estimate would be 14.3% (0.8/0.7).

The energy-normalized intensity is unaffected by the methane composition assumption, since it's not used in any part of the computation for this metric, which we now highlight in the manuscript.

If we use the applicable basin-specific composition estimates from Burdeau et al. 2025, the gas-normalized intensity increases from 2.6% to 2.9% for the Permian Basin (71.5% CH4 comp assumption) and from 12.1% to 16.5% in the San Joaquin Basin (58.6% CH4 composition assumption). So the absolute change for the Permian Basin would be 0.3%, and the percent change relative to the original estimate is +11.9%. For the San Joaquin Basin, the absolute change is 4.4%, and the relative change is +36.6%. The energy-normalized intensities would remain unchanged. To account for the other regions, we use gas compositions from US basins presented in Burdeau et al. (2025) that have comparable fluid production (ie., gas-dominant, oil-dominant, mixed production) to calculate adjusted loss rate metrics. We hope these following changes address the main concerns of the reviewer:

Lines 225-231: "We assume a methane gas composition in natural gas of 80% for loss rate calculations. Assumptions on the methane gas composition directly impact the resulting loss rate calculations and scale inversely to increasing gas composition. We test the sensitivity of our loss rate estimates using methane gas composition values from spatially-explicit estimates for the US (Burdeau et al., 2025) and approximate gas compositions for non-US regions using US basins with similar fluid production characteristics (Table S7). Energy intensity metrics do not incorporate assumptions of methane gas composition into their calculations and are therefore unaffected."

New Table S7 in the SI:

"Table S7: Sensitivity of methane loss rate calculations using assumptions of methane gas composition based on spatially-explicit estimates from Burdeau et al. (2025) for the US. For non-US regions, we choose methane compositions that reflect the fluid production of the basins. For Amu Darya -TKM/UZB, we assume the same methane gas composition as the Appalachian basin (i.e., over 95% of production from gas). For the Zagros Foldbelt, we assume the same gas composition as the San Joaquin. For the Eagle Ford, we use the gas composition provided for the Gulf Coast (Burdeau et al., 2025)."

Region	MethaneSAT loss rates [95% c.i.]	Assumed methane gas composition	Adjusted methane gas composition	Adjusted MethaneSAT loss rate [95% c.i.]
Eagle Ford	2.4% [1.4 – 3.4%]	0.80	0.79	2.4% [1.4 – 3.4%]
Permian	2.6% [1.9 – 3.5%]	0.80	0.72	2.9% [2.1 – 3.9%]
San Joaquin	12.1% [8.9 – 16.0%]	0.80	0.59	16.5% [12.2 – 21.8%]

Amu Darya - TKM	2.9% [2.1 – 3.7%]	0.80	0.90	2.6% [1.9 – 3.3%]
Amu Darya - UZB	3.7% [2.7 – 5.0%]	0.80	0.90	3.3% [2.4 – 4.5%]
Zagros Foldbelt	18.6% [13.4 – 23.8%]	0.80	0.59	25.4% [18.3 – 32.5%]

Point #4: *[Page 17, lines 491-496] You note that MethaneSAT underestimates methane emissions relative to EDGAR for the Amu Darya and Zagros Foldbelt basins, shown in Figure 6. Could you elaborate on potential reasons for this discrepancy? At present, no discussion is provided. In addition, on line 496 you reference Figure 7 when discussing this underestimation relative to EDGAR; however, there are only six figures, and this appears to be a reference to Figure 6.*

EDGAR employs a "bottom-up" inventory methodology in which total methane emissions are estimated by applying emission factors (e.g., methane emissions per unit of oil production) to corresponding activity data (e.g., total oil output). This methodology follows the guidelines of the Intergovernmental Panel on Climate Change (IPCC) and incorporates country-specific oil and gas methane emission factors based in part on the IPCC Tier 1 default values, thereby ensuring consistency, completeness, and comparability across countries (https://edgar.jrc.ec.europa.eu/methodology). The Tier 1 default emission factors generally assume higher methane intensities for oil systems—including venting, fugitive emissions, and flaring—than for gas systems (see https://www.ipcc-nggip.iges.or.jp/public/2006gl/pdf/2_Volume2/V2_4_Ch4_Fugitive_Emissions.pdf). As a result, methane emissions may be overestimated in regions dominated by oil production when regional conditions and technological characteristics—such as high-efficiency flaring, frequent leak detection and repair, and advanced methane capture systems—are not adequately represented. Consistent with this interpretation, recent studies have reported comparatively higher EDGAR methane emission estimates for oil systems (e.g., Scarpelli et al., 2025; https://doi.org/10.5194/essd-17-7019-2025).

We have added new text in the Results to briefly highlight the reason for this difference to Edgar, and have also corrected Figure labels within the main text.

Lines 567 – 571: "Across districts in the Zagros Foldbelt region we find consistent agreement, and even underestimation, of methane emissions from MethaneSAT compared to EDGAR (Fig. 6). In Iran, top-down inversion studies have reported methane emissions lower than EDGAR and closer to UNFCCC inventories (Maasakkers et al., 2019), with discrepancies likely arising in part from differences in the representation of oil and gas emissions and EDGAR's use of generalized emission factors (Crippa et al., 2024)."

For Figure 1, I found the tick label font size and inset text font size to be a bit small and blurry. Please ensure the final figures are clear.

Figure 1 has been replaced with a high-resolution version

I believe Figure 4 is missing a legend to indicate which part of the bars represent oil and gas vs. non-oil and gas emissions. If following could be the non-oil and gas emissions, but this is not indicated in Figure 4.

Legend has been added to clarify a similar oil/gas versus non-oil/gas breakdown for the figure

Page 2, line 52, I think a citation to Veefkind et. al. 2012 for when you introduce TROPOMI would be nice here for completeness.

Agreed – we have added the citation to the relevant section

Online 64, page 2, you need to remove the period after "(i.e., 220 × 440 km2)".

Period has been removed

Page 3, line 79, I believe there is a placeholder "refer to Zhan et. al. 2020" that made it into the final preprint. I believe there should just be a citation to Zhang (not Zhan) et. al. 2020 here.

Placeholder removed and replaced with correct citation

Page 3, line 85, you've got another placeholder for citing Shen et. al. 2022, ACP still in here.

Placeholder removed and replaced with correct citation

Another placeholder citation on Page 3, Line 88.

Placeholder removed and replaced with correct citation

For Figures S3 and S4, the current captions refer to "Sentinel-5P" as the source of SRON-TROPOMI super-emitter detections. For clarity, these should identify that the TROPOMI instrument on the Sentinel-5P satellite provides the methane observations from which plume detections are derived. Moreover, please include formal references and citations for all datasets used in all panels of these figures.

Captions of Figures S3 and S4 adjusted to correctly reference the instruments used for the methane plume detections. We have also included formal references for all the point source imagers in the figure.

There are grammatical and typographical errors in the manuscript that need to be addressed before the article is published, but did not hinder the review process.

We have reviewed the manuscript for typographical and grammatical errors

Response to Reviewer #2

General Comment

This manuscript presents regional methane emissions and intensity estimates derived from MethaneSAT observations across six major oil and gas basins. The dataset is novel and timely, and the comparison with bottom-up inventories and other top-down studies is valuable. The policy relevance of production-normalized methane intensity metrics is also well aligned with ongoing international methane mitigation efforts.

However, while the dataset is strong, the manuscript would benefit from substantial restructuring and clarification to improve scientific framing, methodological transparency, and global balance. At present, the paper reads more as a capability demonstration of MethaneSAT rather than as a clearly articulated scientific investigation. Several methodological choices—particularly those related to sectoral disaggregation and spatial aggregation of prior inventories—require stronger justification. I therefore recommend major revision before the manuscript can be considered for publication.

Major Comments

Point #1: *Scientific Framing and Study Objective*

The Introduction provides extensive background but does not clearly articulate the central scientific question addressed by this study. It remains unclear whether the primary aim is to demonstrate MethaneSAT capability, quantify basin-scale emissions, reconcile top-down and bottom-up discrepancies, or analyze jurisdiction-level intensity differences. A stronger problem-driven framing would significantly improve coherence.

We agree with the reviewer that our Introduction does not clearly outline out research objectives and the overall aim of our study. We have made various edits throughout the Abstract, Introduction, and Discussion/Conclusions to better highlight the main goals of this work which are centered over a demonstration of MethaneSATs capabilities with the added benefit of provided new emissions insights into six high-producing regions of the world.

We hope the following changes address the reviewers' concerns:

Lines 20-21: "Here, we use satellite observations from MethaneSAT (2024–2025) to characterize methane emissions from six oil and gas producing regions as a demonstration of MethaneSAT data capabilities."

Lines 62-68: "Area flux mappers provide basin-scale emission estimates at coarse spatial resolution, while point-source imagers offer fine spatial detail but are primarily sensitive to the largest emitters, leaving a gap in the ability to resolve the full distribution of emissions at high resolution across basin-scale domains.

MethaneSAT, which operated between March 2024 and June 2025, was designed to provide methane observations at intermediate spatial scales, with a native sampling resolution of ~100 × 400 m² and wide swath coverage (~220 – 440 km) suitable for basin-scale mapping (Jacob et al., 2022)."

Lines 94 - 97: "In this paper, we demonstrate the capabilities of MethaneSAT using a compilation of observations from six distinct regions of the world encompassing the Permian oil and gas basin, the Eagle Ford oil and gas basin, the southeastern portion of the San Joaquin Valley, Turkmenistan and Uzbekistan sections of the Amu Darya oil and gas basin, and the Zagros Foldbelt in Iran and Iraq."

Lines 101 – 104: "We also analyze oil and gas normalized intensities for oil and gas methane emissions and additionally apply this analysis across administrative boundaries. Finally, we perform a detailed county/district level analysis of MethaneSAT derived emissions, highlighting the benefits of high-resolution methane emissions data, and compare those estimates to bottom-up inventories."

Lines 586 – 593: "We demonstrate MethaneSAT's ability to deliver satellite-based quantification of methane emissions across six major oil and gas producing regions, leveraging its high precision, high-resolution observations and wide mapping domains (~220 - 440 km swaths). These capabilities enable measurement-based constraints that complement bottom-up inventories, reveal spatial emission patterns and potential new hotspots, and support targeted mitigation strategies (Jacob et al., 2022; Saunois et al., 2025; Shen et al., 2023). The value of this observing system is particularly evident in the Amu Darya – TKM region, where our analysis reveals 5-8 times higher emissions relative to existing bottom-up inventories for the full observation domain (Fig. 4), and 15–62 times higher across four of the top five emitting jurisdictions (Fig. 6)."

Lines 656 – 659: "Our results demonstrate basin, sub-basin and individual jurisdictional-scale emission insights derived using the relatively short operational lifetime of MethaneSAT towards advancing the state of emission quantification to further support and motivate methane mitigation action from the oil and gas sector."

Point #2: *Methodological Transparency and Placement*

Key elements of the inversion-based emission product are deferred to appendices, while the main text provides only brief descriptions. Given that the study's conclusions rely fundamentally on MethaneSAT-derived emissions, the main text should more clearly summarize: Core inversion assumptions, Treatment of atmospheric transport and meteorology, Temporal representativeness of aggregated scenes, Structural sources of uncertainty. At present, readers must consult external references or appendices to understand critical methodological aspects.

To better present our underlying methods, we have moved our Appendices A and B to the Methods section and revised the language surrounding the MethaneSAT CORE inversion

process, including assumptions related to atmospheric transport and meteorology. We have also rewritten sections relating to the uncertainty calculations for all steps of MethaneSAT emissions estimates. For the question on temporal representativeness, we note edits and new analysis to address this concern in a later response to this reviewer.

We hope that the following changes address the reviewers' concerns:

Appendix A rewritten and relocated to Lines 108-142: "Methane emissions inversions from MethaneSAT data produce 0.04° × 0.04° (i.e., 4 × 4 km2) resolution methane emission maps of total methane emissions at spatial scales of roughly 220 × 440 km^2 from a single overpass (i.e., a "collection"). The satellite is equipped with a pair of Littrow passive imaging spectrometers that measure the column-averaged dry-air mole fraction of methane (i.e., XCH4) at a resolution of ~110 m × 400 m at nadir with a precision of 2.5- 5.5 ppb at 2 × 2 km^2. Methane emissions are estimated from MethaneSAT column averaged mole fractions of methane (XCH_4) using the Column Observations to Regional Emissions (CORE) inversion framework, which generates the MethaneSAT Level-4 emissions product. CORE relates observed methane columns to surface fluxes through a linear forward model

$$Z = J_{int} s_{int} + J_{ext} s_{ext} + (z_{prior} + Ab) + z_{topo} + z_{bg}$$

where z is the vector of observed XCH_4 values, J is the Jacobian matrix describing the sensitivity of each observation to surface emissions, s represents methane emission rates within the interior and exterior domains, z_{prior} is the prior methane column used in the Level-2 retrieval, A is the averaging kernel, and b is a background offset parameter.

The source–receptor relationship represented by J is computed using the Stochastic Time-Inverted Lagrangian Transport (STILT) model (Fasoli et al., 2018; Lin et al., 2003) driven by meteorological fields from the Global Forecast System (NOAA Institutional Repository, 2026). STILT simulates backward particle trajectories from observation locations to quantify the sensitivity of each observation to upwind methane emissions. STILT footprints extend up to 28 hours back in time from the satellite observation, which is the ventilation time scale for the observed region size in typical wind conditions, while assuming constant emissions during this time.

MethaneSAT Level-3 observations are aggregated to 2 × 2 km^2 pixels prior to inversion to reduce measurement noise and computational cost. Emissions are estimated on a 4 × 4 km^2 grid within an interior domain defined by contiguous regions of valid observations, while potential emission sources extending up to 300 km beyond the observed domain are included to represent inflow contributions through atmospheric transport. The background methane column is represented as the retrieval prior plus an additive offset parameter scaled by the averaging kernel derived from the Level-2 methane retrieval (Chan Miller et al., 2024). Exterior emission sources are clustered according to the similarity of their transport footprints to reduce the dimensionality of the inverse problem.

Model parameters are estimated using Bayesian inference with state vector $\theta = (s_{int}, s_{ext}, b)$. Posterior samples are generated using the Stan probabilistic programming framework (Carpenter et al., 2017) with the No-U-Turn Sampler (Hoffman and Gelman, 2011), an adaptive Hamiltonian Monte Carlo algorithm (Neal, 2011). Observation uncertainty is represented by a constant standard deviation of 11 ppb, and emission rates are assigned lognormal prior distributions. Posterior mean emission rates provide the estimated flux for each grid cell, and uncertainty on the total dispersed area emissions is the 95% confidence interval from the posterior distribution (n=4,000), with an additional 20% uncertainty added to account for assumed uncertainty in the static parameters in the input GFS weather data used for the inversions."

Appendix B rewritten and relocated to Lines 145-172: "Individual MethaneSAT emissions estimates (i.e., a MethaneSAT scene or emissions map) represent methane emission estimates up to 28 hours back in time and vary in their spatial dimensions depending on the viewing geometry of the satellite. Nadir viewing observations produce up to ~220 km wide scenes while off-nadir observations produce up to ~440 km wide scenes. The MethaneSAT platform had an agile observing mechanism with off-nadir viewing at up to 40 degrees on one side of its observing track. We aggregate multiple MethaneSAT scenes together over the same regions to produce a spatially explicit estimate of methane emissions with increased temporal and spatial extents. To do this, we reproject all MethaneSAT emissions estimates onto a common global 0.04° × 0.04° grid (Fig. S1) using an equal-area weighting approach that preserves total methane mass among the individual scenes. Then, we average the methane emission rates over each cell for each overlapping scene and combine to produce an aggregated methane emission heatmap. We apply the same approach using the median during aggregation as an additional test of sensitivity and find broad consistency between the two approaches (Fig. S10). We also test the sensitivity of MethaneSAT aggregated emissions estimates to the removal of single scenes and find that estimates are robust among the six regions (SI – Section 2, Fig. S12). We additionally consider any impacts from seasonal variability in our aggregated emissions estimates using 2022 monthly inversions data from TROPOMI (Pendergrass et al., 2025) to better compare to annual emissions estimates from top-down satellite inversions or bottom-up inventories (SI – Section 2).

We perform intercomparisons of total methane emissions estimates to other spatially explicit methane emissions data from both bottom-up and top-down methodologies. In all intercomparisons, we match the spatial domains to ensure that the same regions are being compared. In addition to total methane emissions, we also produce comparisons of available literature-based emissions from different sectors (i.e., oil and gas and non-oil and gas emissions). From the bottom-up inventories, we specifically compare MethaneSAT to the EPA-GHGI (Maasakkers et al., 2023) for observations in the US, and to EDGAR - version "EDGAR_2025_GHG" (Crippa et al., 2024) and CAMS v6.2 (Granier et al., 2019) for regions outside of the US. The EPA-GHGI provides annual estimates of methane emissions for 2020, while EDGAR and CAMS v6.2 both report annual emissions for 2024. The EPA-GHGI and EDGAR provide emissions estimates for member countries under the UNFCCC. Other bottom-up inventories that are used as prior information for satellite-based inversions include the Global Fuel Exploitation Inventory (GFEI v2) (Scarpelli et al., 2022) and CAMS v6.2 (Granier et al., 2019). Our comparisons to top-down satellite-based observations vary by region and are presented later in the Results section."

Point #3: *Sectoral Disaggregation and Prior Dependence*

Sectoral attribution is based on proportional redistribution using composite prior inventories. While pragmatic, this approach implies that sectoral breakdowns are structurally dependent on prior spatial patterns rather than independently resolved from observations. Because sectoral results and methane intensities are central conclusions of the paper, the manuscript should: More explicitly acknowledge this dependence, Clarify the structural uncertainty associated with prior selection and spatial aggregation, Strengthen the justification for prior resolution choices (e.g., 0.4° aggregation outside the U.S.). This point is especially important for interpreting cross-region intensity differences.

We agree that more detail is added to discuss the structural uncertainties related to the use of a spatially-explicit prior in our sectoral attribution of methane emissions, and to justify our selection of inventories used within the composite prior and modification of

the resolution for oil and gas emissions in regions outside of the US. Although we do accept that there are inherent uncertainties in the sectoral attribution process, we also note that MethaneSAT emissions estimates do not utilize a prior emission inventory to spatially allocate methane emissions, which is uncommon among satellite-based inversions of methane emissions and adds a degree of independence. We have added new sections in the SI to address these points and have included new figures and tables to support the selection of priors and the modification of the native prior inventory resolution for oil and gas estimates outside of the US.

In short, we estimate a literature-based proportion of oil and gas to total methane emissions for each region through a combination of bottom-up inventories and satellite inversions. We incorporate this proportion into our current sensitivity analysis (SI Figures S6-S8) that shows the variations in sectoral emissions using different combinations of inputs for our composite prior inventory, and subsequent variations of the native prior inventory resolutions for oil and gas methane emissions. We use this literature-based proportion to inform our decisions in the manuscript regarding our selection and treatment of the composite prior inventories. For example, we find that the decreased spatial resolution for oil and gas emissions improves agreement to the literature-based proportions in non-US regions, with negligeable changes to the US-based regions. We believe that these additional changes greatly improve the manuscript.

We hope the following modifications address the reviewers points:

Lines 187-193: "For any region and sector, we combine emissions estimates from two bottom-up inventories with Carbon Mapper distinct point sources to produce the composite dataset. For regions within the US, we use the EPA-GHGI and EDGAR as inputs for non-oil and gas sources, and the EI-ME and EDGAR for oil and gas sources. For regions outside of the US, we use CAMS v6.2 and EDGAR as inputs for non-oil and gas sources, and the GFEI v2 and EDGAR as inputs for oil and gas sources. Other combinations of these bottom-up inventories, and their impacts on the resulting sectoral breakdown of emissions, are provided in the SI (Fig. S7; Fig. S8) with further explanation in the SI – Section 1.1."

Lines 195-200: "To better account for regions where granular oil and gas infrastructure data is limited (i.e., regions outside of the US), we spatially aggregate oil and gas methane emissions estimates from the composite prior by a factor of four (i.e., from the native 0.1° x 0.1° resolution to 0.4° x 0.4°) while conserving the mass of emissions. A sensitivity test of this approach shows improved agreement in the sectoral proportions of emissions for non-US regions compared to a compilation of estimates from literature, while showing little to no improvement for regions in the US (SI – Section 1.2)."

Lines 623-626: "Sectoral attribution is applied as a post-inversion step using a composite prior inventory drawn from multiple spatially explicit datasets supplemented by global point source data from Carbon Mapper (2025). This approach improves sectoral allocation, especially for regions where information on oil and gas emissions data is sparse and information from one inventory can account for discrepancies in another (SI – Section 1.1, Fig. S5)."

Newly added sections: SI Section 1.1: "Selection of inventories used for composite prior" and SI Section 1.2 "Oil and gas estimates for non-US regions"

Revised Figure S6 in the SI:

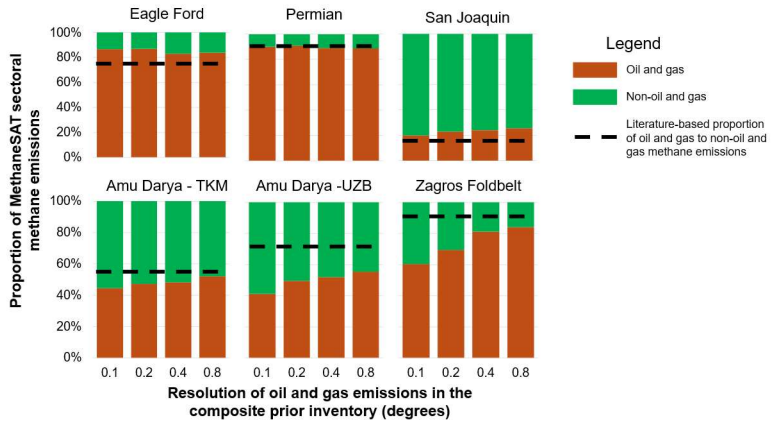

"Fig. S6: Impacts of varying the resolution of the oil and gas sectoral emissions from the composite prior inventory used to disaggregate methane emissions estimates from MethaneSAT. Results of the sensitivity test for all six regions are shown. The dashed black line indicates the literature-based proportion of oil and gas to non-oil and gas methane emissions in the six regions. For the US regions (top row), the chosen resolution used for sectoral disaggregation is 0.1 degrees. For non-US regions (bottom row), we use a resolution of 0.4 degrees."

Revised Figure S7 and S8 in the SI:

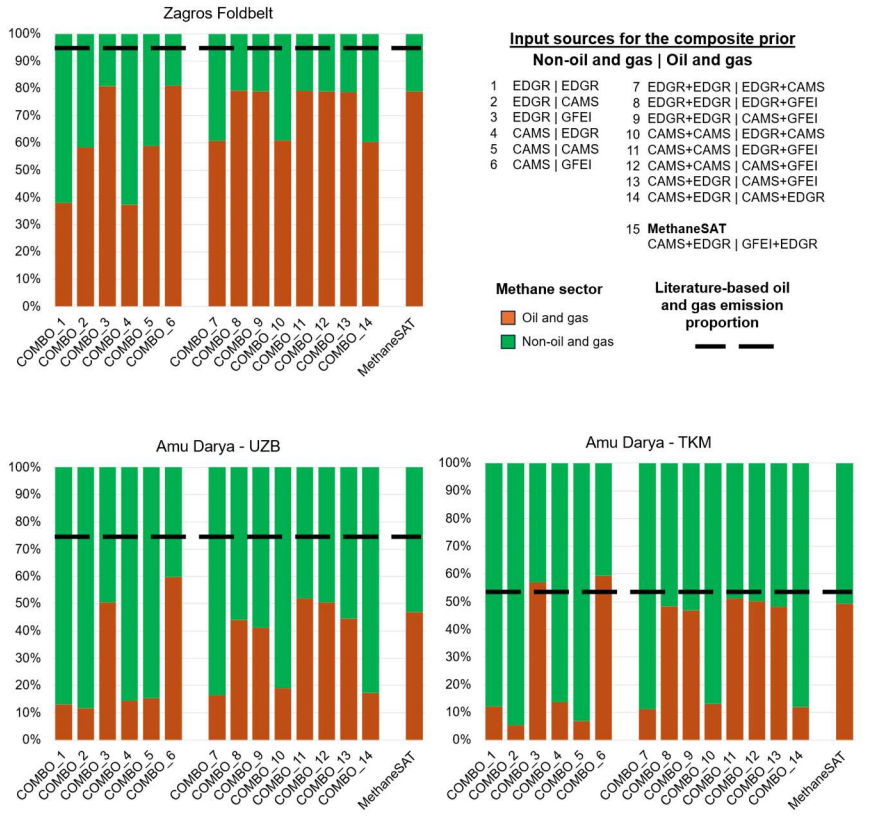

"Fig. S8: Impacts of varying the input data used in the stacked prior inventory to disaggregate methane emissions from the MethaneSAT observations for regions outside of the US. The impacts of the inclusion

of Carbon Mapper point sources are also not shown. The dashed black line indicates the literature-based proportion of oil and gas to non-oil and gas methane emissions in the six regions."

New Table S4 in the SI:

"Table S4: Studies and data sources used in the calculation of a literature-based proportion of oil and gas emissions which is explained in the SI Sections 1 and 2. Also indicated in the table is the respective name for the spatially-explicit methane emissions estimate (if applicable), a broad descriptor of the methodology used to obtain the methane emission estimate, a breakdown of the methane sectors included in the estimate, and the latest year represented within the dataset."

Study	Data source name	Method	Sectors included	Latest year
(Maasakkers et al., 2023)	EPA-GHGI	Bottom-up	All	2018
(Omara et al., 2024)	EIME	Bottom-up	Oil and gas	2023
(Granier et al., 2019)	CAMS v6.2	Bottom-up	All	2024
(Crippa et al., 2024)	EDGAR_GHG_2025	Bottom-up	All	2024
(Scarpelli et al., 2022)	GFEI v2	Bottom-up	Oil and gas, coal	2019
(East et al., 2025)	-	TROPOMI	All	2023
(Shen et al., 2023)	-	TROPOMI	Oil and gas, coal	2019
(Worden et al., 2022)	-	GOSAT	All	2019
(Lu et al., 2023)	-	GOSAT	All	2019
(Nesser et al., 2024)	-	TROPOMI	All	2019

New Table S5 in the SI:

"Table S5: Literature-based estimates of oil and gas and non-oil and gas emissions within the spatial domains of all six regions. The resulting proportions are used to inform the selection process of inputs used for the composite prior, and to support the use of decreasing the resolution of bottom-up inventories."

Region	Literature-based oil and gas estimate (t/h)	Literature-based non-oil and gas estimate (t/h)	Literature-based proportion of emissions (oil and gas / non-oil and gas)
Eagle Ford	46.9	14.4	77 / 23
Permian	290	23.8	92 / 8
San Joaquin	16.1	82.7	16 / 84
Amu Darya - TKM	57.9	48.6	54 / 46
Amu Darya - UZB	94.4	32.4	74 / 26
Zagros Foldbelt	310	16.0	95 / 5

Point #4: *Temporal Representativeness of Aggregated Emissions*

The study aggregates 33 MethaneSAT overpasses over approximately one year, yet there is limited discussion of seasonal representativeness or meteorological variability. It is unclear to what extent the aggregated emissions can be interpreted as annual averages. Further clarification is needed to present in this work.

To better present the seasonal representativeness and meteorological variability of MethaneSAT emissions estimates, we have added new figures and tables in the SI alongside additional text in the Methods and Results sections that account for any seasonal biases the daily aggregated MethaneSAT emissions may contain. We have also added a new Section in the SI (Section 2: Aggregation of MethaneSAT scenes and seasonal variability) to further discuss the impacts of seasonal patterns on the emissions, in addition to other factors. Overall, the six regions show varied changes in emissions after accounting for the seasonal timing of retrievals, but none produce emission estimates beyond our stated 95% confidence intervals. We feel that the following changes to the manuscript and additional analysis contained in the SI address the reviewers main concerns.

Lines 145-151: "Individual MethaneSAT emissions estimates (i.e., a MethaneSAT scene or emissions map) represent methane emission estimates up to 28 hours back in time and vary in their spatial dimensions depending on the viewing geometry of the satellite. Nadir viewing observations produce up to ~220 km wide scenes while off-nadir observations produce up to ~440 km wide scenes. The MethaneSAT platform had an agile observing mechanism with off-nadir viewing at up to 40 degrees on one side of its observing track. We aggregate multiple MethaneSAT scenes together over the same regions to produce a spatially explicit estimate of methane emissions with increased temporal and spatial extents."

Lines 156-160: "We also test the sensitivity of MethaneSAT aggregated emissions estimates to the removal of single scenes and find that estimates are robust among the six regions (SI – Section 2, Fig. S12). We additionally consider any impacts from seasonal variability in our aggregated emissions estimates using 2022 monthly inversions data from TROPOMI (Pendergrass et al., 2025) to better compare to annual emissions estimates from top-down satellite inversions or bottom-up inventories (SI – Section 2)."

Lines 294-302: "The seasonal representativity of the individual scenes are discussed in the SI – Section 2 (Fig. S13). We aggregate these single scenes together to form regional estimates of methane emissions. In the US, the aggregated MethaneSAT observation domains capture 99% of total onshore oil and gas production for 2024 in the Permian and San Joaquin regions, and 66% of onshore production in the Eagle Ford (Fig. S9) (Wood Mackenzie, 2025). Outside of the US, the aggregated MethaneSAT observation domains cover 58% of total onshore oil and gas production in the Zagros Foldbelt, and 79% of total onshore oil and gas production from the Amu Darya oil and gas basin from the combined observations in Uzbekistan and Turkmenistan (Fig. S9). Cumulatively, the six regions account for 11% of global onshore oil and gas production for 2024 (Wood Mackenzie, 2025)."

Lines 400-402: "We find no strong seasonal biases in our methane emissions estimates for the Eagle Ford (SI – Section 2, Table S6), implying that the differences between top-down estimates are reflective of the observed methane emissions."

Lines 408-413: "We find higher emissions from non-oil and gas sources (i.e., 97 t h^{-1}) within the San Joaquin region compared to older satellite-based estimates (Lu et al., 2023; Worden et al., 2022), additionally noting that the aggregated MethaneSAT estimates may underestimate emissions by ~10% based on the seasonal timing of the scene collections (SI – Section 2; Table S6). We further note that our measurements were performed during daylight hours, which would also influence comparisons with annual average inventory estimates for the San Joaquin (SI – Section 2)."

Newly added section: SI Section 2 "Aggregation of MethaneSAT scenes and seasonal variability"

Newly added Figure S12:

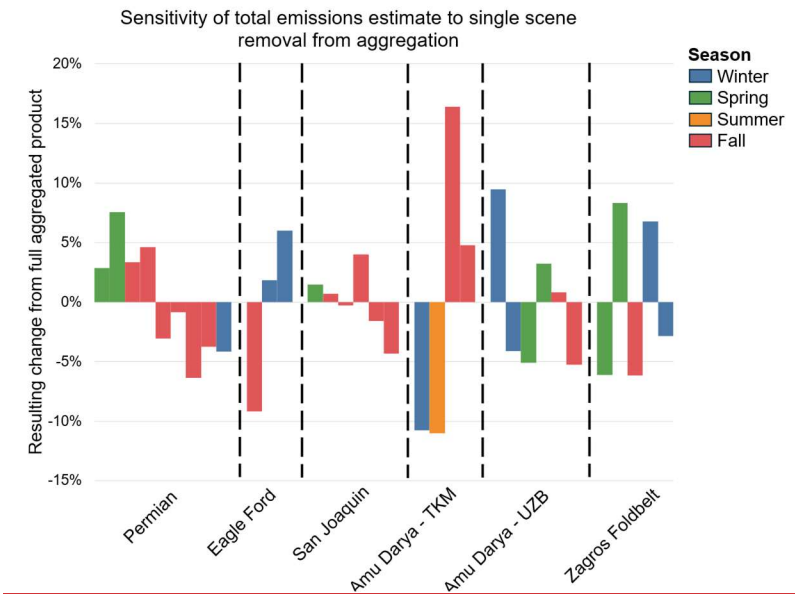

"Fig. S12: Resulting variation in MethaneSAT aggregated emissions estimates after single scenes from the aggregation process. The bars are colored according to the season from which the MethaneSAT observations were obtained. The percentage differences are calculated based on the same spatial domain since the removal of scenes can vary the extent of the aggregated output boundary."

Newly added Figure S13:

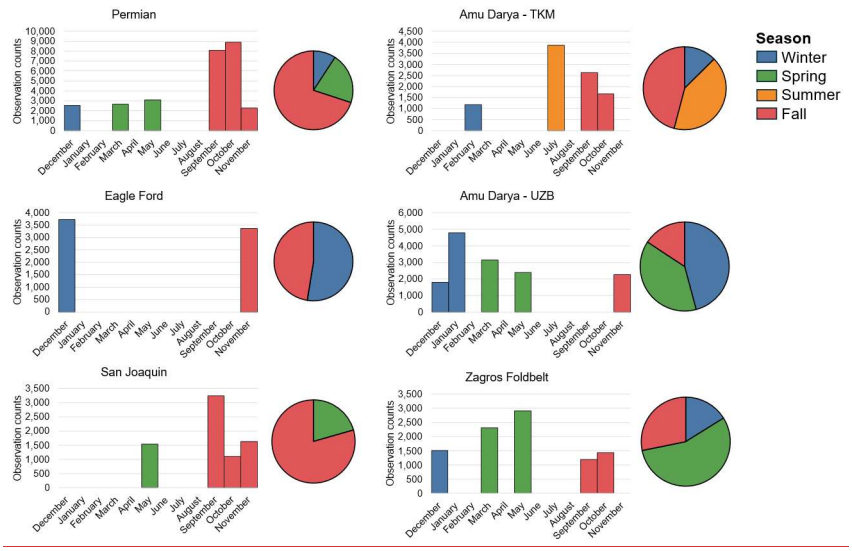

"Fig. S13: Observation counts from individual MethaneSAT scenes for all six regions over different months. Pie charts represent the accumulated observations by different seasons."

Newly added Figure S14:

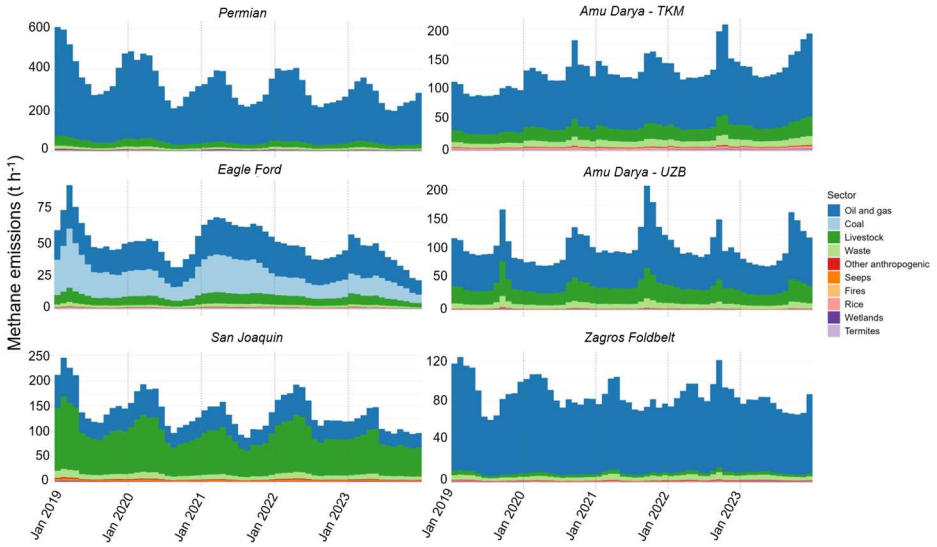

"Fig. S14: Monthly trends in sectoral methane emissions for 2019-2023 from gridded estimates derived from global TROPOMI observations using the localized ensemble transform Kalman filter (CHEEREIO v1.3.1) (Pendergrass et al., 2025). Seasonal emissions from Pendergrass et al. (2025) are mapped at their native resolution of 200 × 250 km and calculated using an equal area weighting approach for the aggregated MethaneSAT spatial domains."

Newly added Table S6:

"Table S6: Aggregated MethaneSAT adjusted according to seasonal correction factors calculated using monthly methane emissions trends by sector from Pendergrass et al (2025). The 95% confidence intervals on the adjusted MethaneSAT emissions are proportional to the confidence intervals on the current MethaneSAT total emissions estimates."

Region	MethaneSAT total emissions (t h^{-1}) [95% c.i.]	Seasonal correction factor using sectoral methane emissions from TROPOMI	Adjusted MethaneSAT emissions (t h^{-1}) [95% c.i.]
Eagle Ford	114 [83 - 149]	1.02	117 [85 - 152]
Permian	454 [351 - 563]	1.14	516 [399 - 640]
San Joaquin	127 [95 - 162]	1.09	138 [104 - 177]
Amu Darya - TKM	188 [141 - 239]	0.89	168 [126 - 213]
Amu Darya - UZB	192 [146 - 242]	1.05	201 [153 - 254]
Zagros Foldbelt	251 [189 – 321]	0.95	238 [180 - 305]

Point #5: *Global Framing vs. Regional Emphasis*

While the manuscript is framed around "major oil and gas basins," the selected regions represent a limited subset of global production areas and include a strong emphasis on U.S. basins. Given that MethaneSAT is a global observing system, readers may naturally interpret the results as indicative of broader global oil and gas emission patterns.

The authors are encouraged to clarify: the rationale for regional selection, the representativeness of these basins relative to global oil and gas production, whether the conclusions are intended to reflect global variability or only the specific observed regions. If MethaneSAT observations are not yet globally comprehensive, this limitation should be explicitly acknowledged to avoid overgeneralization. Alternatively, moderating the global framing in the Introduction and Conclusions may help align scope with coverage.

We understand the reviewers concerns on the current global framing of the manuscript and how this can be misleading given that we focus on six regions for the paper. We have adjusted the manuscript to better present this work as a demonstration of MethaneSAT's capabilities with the six regions chosen to represent 1) availability of MethaneSAT data at the time of writing, 2) a diverse sectoral breakdowns of emissions, 3) variable oil and gas production characteristics, and 4) a mix of US and non-US locations. As for the representativeness of these basins relative to global oil and gas production, we have added an additional line of text to clarify that these basins encompass roughly 10% of global oil and gas production which is notable, but not representative of the entire oil and gas industry.

We believe that earlier changes made in response to the reviewers comments address the most of these concerns, specifically relating to the global framing versus

demonstration MethaneSAT capabilities (see Response to Point #1). We additionally highlight the text below that describes the reasoning behind the region selections.

Lines 97-99: "The regions were selected to represent a range of oil and gas production magnitudes, production characteristics (i.e., predominantly oil, gas, or a mixture of production), geography, and presence of non-oil and gas methane sources."

Point #6: *Manuscript Structure and Narrative Coherence*

The manuscript would benefit from improved structural balance and clarity of presentation. At present, some core analytical elements are relatively condensed in the main text, while detailed regional descriptions receive substantial space. A clearer emphasis on the primary analytical framework and synthesis of findings in the main body—while streamlining secondary descriptive material—would enhance readability and better highlight the study's central contributions.

We acknowledge that the manuscript would benefit from increased clarity of presentation, and an overall streamlining of the data to provide a more robust explanation of the underlying methods and reduced emphasis on secondary descriptive content. To address these points, we have moved our Appendices to the main Methods (addressed in response to Point #2), removed descriptive text that does not significantly impact our results/conclusions, and edited text to more concisely outline the main analytical framework. We would also highlight our responses to Point #1 which also address these concerns.

Lines 62-68: "Area flux mappers provide basin-scale emission estimates at coarse spatial resolution, while point-source imagers offer fine spatial detail but are primarily sensitive to the largest emitters, leaving a gap in the ability to resolve the full distribution of emissions at high resolution across basin-scale domains.

MethaneSAT, which operated between March 2024 and June 2025, was designed to provide methane observations at intermediate spatial scales, with a native sampling resolution of ~100 × 400 m² and wide swath coverage (~220 – 440 km) suitable for basin-scale mapping (Jacob et al., 2022)."

Lines 237-244: "Uncertainty in aggregated MethaneSAT emissions estimates is propagated using a Monte Carlo approach. Each emissions cell is represented by 4,000 samples drawn from its MCMC posterior distribution, reflecting mean-level uncertainty in the emissions estimate at that location. Where multiple emissions maps overlap a given cell, 4,000 combined cell-level estimates are generated by repeatedly drawing one value per map and averaging across maps. This Monte Carlo resampling procedure propagates uncertainty through the arithmetic mean without requiring assumptions about the functional form of the resulting distribution. This procedure is applied independently to all subregions defined by unique combinations of overlapping emissions maps (Fig. S2)."

Line 266: "~~99% of total oil and gas production within the Permian oil and gas basin by combining a total of nine MethaneSAT observations with repeat coverage over the Midland and Delaware sub-basins, both associated with most of the oil and production in the larger Permian basin.~~"

Line 272: “~~combines six observations over two distinct regions of the San Joaquin Valley - the Kings and Tulare counties which have been previously identified as regions with elevated methane emissions associated with livestock-related agricultural activity, and the Kern county associated with a mixture of oil and gas activity, landfills, and agricultural activity.~~”

Line 273: “~~Oil and gas production within the San Joaquin basin has been steadily declining over the past four decades (EIA-914 monthly production report, 2025).~~”

Line 284: “~~, with the first productive gas fields discovered around the 1950’s before development continued throughout the 1960’s to 1980’s (Ulmishek, 2004).~~”

Line 286: “~~with periodical investments stimulating modernization in the basin, producing a mixture of legacy and upgraded infrastructure~~”

Lines 296-302: “In the US, the aggregated MethaneSAT observation domains capture 99% of total onshore oil and gas production for 2024 in the Permian and San Joaquin regions, and 66% of onshore production in the Eagle Ford (Fig. S9) (Wood Mackenzie, 2025). Outside of the US, the aggregated MethaneSAT observation domains cover 58% of total onshore oil and gas production in the Zagros Foldbelt, and 79% of total onshore oil and gas production from the Amu Darya oil and gas basin from the combined observations in Uzbekistan and Turkmenistan (Fig. S9). Cumulatively, the six regions account for 11% of global onshore oil and gas production for 2024 (Wood Mackenzie, 2025).”

Line 369: “~~– TKM and Amu Darya – UZB cover 79% of total oil and gas production within the Amu Darya oil and gas basin(Wood Mackenzie, 2025) (Fig. S9) with~~”

Line 402: “~~, implying that the elevated emission observations from MethaneSAT may reflect increasing natural gas production in recent years, especially from the Austin Chalk Play where natural gas production has nearly quadrupled since 2014 (EIA-914 monthly production report, 2025).~~”

Line 413: “~~(Fig. 3), which may reflect changes in the dairy industry for the region. While oil and gas production has declined in recent decades, milk production has grown 153% in the state of California since the early 1980’s, with most of the growth occurring within Tulare county (Barrowman et al., 2025).~~”

Line 425: “~~However, this contradicts production trends in both Iran and Iraq which both show increasing gas production over the past decade based on the International Energy Agency(IEA, 2025) (Iraq – Countries & Regions, 2025; Iran – Countries & Regions, 2025).~~”

Minor Comments

Line 79,84,88: the right references should be cited.

Correct references are now cited

Line 115: “significantgrowth” → missing space.

Space added on this line

Line 146: “upto” should be written as “up to.”

Space added on this line

Line 147: “it’s observing track” should be “its observing track.”

Language corrected

Line 685: Insert the emission link?

The Data Availability section has been revised to direct readers to the open access data for L1b, L2, L3, and L4 products.

Inconsistent use of “95% c.i.” vs “95% CI.”

Confidence intervals are now consistently displayed as “95% c.i.” throughout the main text and SI

Hyphenation inconsistencies (e.g., “gas-production normalized” vs “gas-production-normalized”).

Hyphenation adjusted to be consistent throughout the text

Several web-based references (e.g., IEA website) lack formal citation formatting and access dates consistent with ACP style.

Citation formatting corrected

Ensure unit consistency throughout (t/h, kg CH_4/GJ formatting).

Unit consistently corrected for the main paper and SI

Some URLs appear directly in text; these should follow ACP referencing guidelines.

In-text citation formatting corrected